Desalination and Water Treatment
www.deswater.com

doi: 10.1080/19443994.2013.793922

52 (2014) 1440–1447
February

Taylor & Francis
Taylor & Francis Group

Terbium adsorption onto polyhydroxyethylmethacrylate–hydroxyapatite composite and its modified composition by phytic acid

Recep Akkaya

Vocational School of Health Services, Cumhuriyet University, Sivas 58140, Turkey
Tel. +90 3462191010/1341; Fax: +90 3462191256; email: rakkaya@cumhuriyet.edu.tr

Received 22 March 2012; Accepted 17 March 2013

ABSTRACT

Hydroxyapatite (Hap) was entrapped in poly(hydroxyethylmethacrylate) P(HEMA) by direct polymerization and P(HEMA–Hap) was obtained in aqueous solution. Phytate (phy) was immobilized by phytic acid (phy) modification onto the poly(hydroxyethylmethacrylate–hydroxyapatite), P(HEMA–Hap). The adsorptive features of P(HEMA–Hap) composite and its modified form P(HEMA–Hap)–phy, were investigated by using Tb analogues, rare earth elements (REE), by isotopic tracer method, ^{160}Tb was used as the radiotracer. It was observed that P(HEMA–Hap) composite had a higher affinity for Tb^{3+} than bare Hap, as well as its modified composition P(HEMA–Hap)–phy. Adsorption data obtained, fitted well to the classical Lagmuir, Freundlich, and Dubinin–Radushkevich (D–R) sorption models. Changes in enthalpy and entropy values showed that the overall adsorption process was endothermic ($\Delta H > 0$), increasing entropy ($\Delta S > 0$), and spontaneous ($\Delta G < 0$), as expected. The adsorption kinetics following the pseudo-second order model indicated that the rate-controlling step was the chemical adsorption. Reusability of the adsorbent was also investigated and it was found that the adsorbent could be used at least for five times.

Keywords: Adsorption; Composite; Poly(hydroxyethylmethacrylate); Hydroxyapatite; Terbium

1. Introduction

In the nature, the rare earth elements (REE) are usually found together with several elements, such as phosphates, carbonates and silicate minerals. In the past decade, the aqueous chemistry of the REE has received a growing interest [1–5]. Terbium is an important member of the REE. In industry, Tb^{3+} is used in high technology applications, environmental chemistry, and in space research. Besides its industrial importance, the removal/recovery of Tb^{3+} is also important because of its toxicity [6,7] and its presence in nuclear waste [8]. The abundance of ^{160}Tb is in minerals could reach 100% and its halflife, 72d, is long enough for experimental manipulations. An extraction resin containing 1-hexyl-4-ethyloctyl isopropylphosphoric acid (HEOPPA) has been found to be suitable for the separation of Tb^{3+} and heavy rare earth ions from hydrochloric acid solution [9]. Furthermore, studies involving Tb^{3+} adsorption onto clay modified with humic/fulvic acid clay materials have also been performed [10].

Adsorption is a promising technique because of its high efficiency, easy handling, and the availability of different adsorbent materials [11,12]. Although P(HEMA) is a nonadsorbent and hydrophilic polymer [13–16], many P(HEMA) containing composites have been demonstrated to serve as good adsorbent composites [17,18]. Hap minerals have also been considered as an ideal low cost metal element adsorbent [19–27] because of their high sorption capacity for metal ions. So far, only a limited number of studies have been performed to modify Hap surface and thereby to improve its adsorption capacity [28–31].

In recent studies, hydrogels–containing adsorbent composites have attracted much attention polymer technology due their better mechanical, thermal and adsorptive properties, and their dimensional stability in comparison with pure polymers or conventional composites [32–34].

A number of polyacrylamide-based composite materials, that is polyacrylamide–bentonite, have been produced and then modified with phytic acid (phy). It has been shown that the modification has improved the adsorbent capacity of the composites to UO_2^{2+}, Th^{4+}, and Pb^{2+} in aqueous media [24]. On the basis of these findings, this study also aimed to improve the adsorbent capacity of P(HEMA–Hap) towards Tb^{3+} by modification with phy. The main aim of this study was therefore to use both P(HEMA–Hap) and a modified form of it, with phytic acid [P(HEMA–Hap)–phy], and to demonstrate their adsorbent capacity, this time, for Tb^{3+}, relative to the adsorbent capacity of Hap *per se*. Adsorptive capacities of Hap, P(HEMA–Hap), and P(HEMA–Hap)–phy were compared using Tb^{3+}. Some physicochemical parameters (pH, concentration, time, and temperature) for the adsorption process were optimized by employing a radiotracer method involving ^{160}Tb. Reusability of P(HEMA–Hap), and P(HEMA–Hap)–phy for the adsorption was also studied. The experiments were always performed in duplicates where ±5% was the limit of experimental error. An equilibration time of 24 h was used for the solution and adsorbent and the temperature of the experiments was always 298 K.

2. Experimental

2.1. Reagents

Arsenazo III (disodium salt) was obtained from Acros. HEMA, EGDMA, Na-phytate, N,N,N′,N′-tetramethylethylenediamine, APS ($H_8N_2O_8S_2$), and Tb_2O_3 were purchased from Sigma Aldrich. Hap was obtained from Sigma in ground and sieved form ranging in particle size from 63 to 125 nm [11].

All experiments were performed in duplicates and the limit of experimental error was ±5% for each of the experiments.

2.2. Preparation of P(HEMA–Hap) composite and its modification by phy

Ten grams of P(HEMA–Hap) was synthesized by bulk polymerization in aqueous medium (20 mL) using 3:1 PHEMA/Hap ratio [two g of Hap and 10 ml HEMA solution, containing 1/3 HEMA (v/v)] This 3:1 ratio of has been found to be optimum, in terms of the cost and effective adsorbent capacitiy, for the preparations of other composites (polymer matrix/natural adsorbents) in previous studies [11,35,36]. In the reaction eight ml EGDMA crosslinker, 500 μg ammoniumpersulphate (APS), and 200 μL TEMED (stock solution) were used. The final reaction mixture was stirred for four h at 25°C. The reaction product, P(HEMA–Hap) composite was washed with distilled water until the effluent attained neutral pH. The composite was then dried at ambient temperature, sieved to a particle −25 mesh sizes.

Its modification by phytic acid, 0.1 g of P(HEMA–Hap) was added into 10 mL of Na-phytate solutions, pH 10, prepared at $4.5 \times 10^{-3}\,mol\,L^{-1}$ concentrations. The adsorbent-solution systems were equilibrated for 24 h at 298 K in a thermostatic water bath. The suspensions were then centrifuged for five min at 3,000 rpm. Phylate concentrations in the supernatants were determined by using a modified precipitation method [24]. P(HEMA–Hap)–phy adsorbent was used for Tb^{3+} adsorption studies. For the process, 11 different solutions, at concentrations ranging from 20 ppm to 2,000 ppm, of Tb^{3+} were prepared. Onto each of the Tb^{3+} solution 0.1 g of P(HEMA–Hap) or P(HEMA–Hap)–phy adsorbents were added. The adsorption experiment was repeated twice.

2.3. Preparation of ^{160}Tb tracer

Eighty milligrams of Tb_2O_3 were subjected to thermal neutron flux irradiation ($7 \times 10^{-11}\,n\,cm^{-2}\,s^{-1}$) in a nuclear reactor (Çekmece Nuclear and Research Centre, Turkey) to obtain ^{160}Tb ($t_{1/2} = 72.3\,d$) with 1 MBq activity. The irradiated sample was dissolved in 5 mL of $1\,mol\,L^{-1}$ HNO_3 and diluted to 20 mL to obtain 50,000 Bq mL^{-1} activities). For the preparation of the tracer stock, a dilution of ^{160}Tb with 250 Bq mL^{-1} was used an activity of. One milliliter of this tracer solution was used for every 10 mL of Tb^{3+} adsorption solution.

2.4. *pH dependence of the adsorption*

The effect of pH on Tb^{3+} ($3.1 \times 10^{-3}\,mol\,L^{-1}$) adsorption onto P(HEMA–Hap) and P(HEMA–Hap)–phy adsorbents was investigated at pH points ranging from one to five.

2.5. *Concentration dependence of the adsorption*

One hundred milligrams of P(HEMA–Hap), P(HEMA–Hap)–phy and Hap were equilibrated with 10 mL stock Tb^{3+} solutions prepared at concentrations ranging from 1.6×10^{-4} to $1.3 \times 10^{-2}\,mol\,L^{-1}$. The adsorbent-solution systems were equilibrated for 24 h at 298 K in a thermostatic water bath. The suspensions were then centrifuged for five min at 2,500 rpm. The initial/final pH values of the solutions were always within the range of 3/5.

Fractional adsorption was determined by gamma-spectrometric method using an NaI(Tl) detector (EG&G ORTEC multi-channel analyzer (Five milliliter aliquots of adsorption samples and a reference solution (5 ml ^{160}Tb tracer) were read in contact geometry collectors (at least 10,000 cpm for the provision of 1% standard error. The adsorbed fraction of Tb^{3+} was then derived from the comparison of ^{160}Tb tracer activities (at 87, 197, 299, 876, 966, and 1,178 keV).

2.6. *Adsorption kinetics*

One hundred milligrams of solid P(HEMA–Hap) and P(HEMA–Hap)–phy were added onto the 50 mL Tb^{3+} solutions. Fifty microliter fractions of the adsorption sample were withdrawn at 0, 1, 2, 5, 10, 15, 30, 60, 120, 240, and 480 min. Tb^{3+} contents were determined as described above. By taking the fact that the suspension volume decreased after taking each of the aliquots, a correction factor was applied to the calculated ion content values.

2.7. *Temperature dependence of adsorption*

One hundred milligrams of P(HEMA–Hap) and P(HEMA–Hap)–phy equilibrated with Tb^{3+} solution at $1.6 \times 10^{-3}\,mol\,L^{-1}$ ($250\,mg\,L^{-1}$), were incubated for 24 h at five different temperature points, 278, 288, 298, 308, and 313 K, to determine the effect of temperature onto ion adsorption.

2.8. *Reusability*

One hundred milligrams of P(HEMA–Hap) and P(HEMA–Hap)–phy were equilibrated, in polypropylene columns (100 mm height × 10 mm i.d., with a glass-wool over its stopcock), with 10 mL of $1.6 \times 10^{-3}\,mol\,L^{-1}$ ($250\,mg\,L^{-1}$) Tb^{3+} solution for 6 h. The amount of adsorbed Tb^{3+} ions was derived from the contents of solutions at equilibrium. P(HEMA–Hap) and P(HEMA–Hap)–phy adsorbent materials were precipitated after the adsorption procedure and was then placed in the column to remove Tb^{3+} ions by washing with 15 mL, $1\,mol\,L^{-1}$ HCl at $0.5\,mL\,min^{-1}$. The complete recovery of the adsorbed Tb^{3+} was verified by determining the amount of Tb^{3+} in the eluents. The columns were then reconstituted with distilled water until the effluents reached neutral pH. The reusability experiments were performed for five times by using duplicate samples.

2.9. *The effect of ionic strength*

One hundred milligrams of P(HEMA–Hap) and P(HEMA–Hap)–phy were interacted with 10 mL of $6.3 \times 10^{-3}\,mol\,L^{-1}$ Tb^{3+} solutions containing 0.01, 0.02, 0.04, 0.08, 0.10, 0.20, 0.25, and $0.30\,mol\,L^{-1}$ of $CaCl_2$ for 24 h. Tb^{3+} ions contents of the eluents were then measured using the process described above.

3. Results and discussion

Structural characterization of P(HEMA–Hap) has been performed in a previous study by P(HEMA–Hap) Fourier transform-infrared spectroscopy (FT-IR), X-ray diffraction (XRD), thermogravimetric analysis (TGA), scanning electron microscope (SEM), and Brunauer–Emmett–Teller (BET)-porosity. Results of SEM and BET have demonstrated clearly that, in comparison with Hap, the composite possessed a rather micro-porous structure. FT-IR, XRD, and TGA spectra have showed a hybrid structure for the composite.

3.1. *pH dependence of Tb^{3+} adsorption*

Adsorption onto P(HEMA–Hap) and P(HEMA–Hap)–phy adsorbents appeared to show a sharp increase above pH 3 (Fig. 1). Maximum Q values obtained at pH points ranging from of one to five were 0.41 and $0.44\,mol\,kg^{-1}$ for P(HEMA–Hap) and 0.34 and $0.52\,mol\,kg^{-1}$ for P(HEMA–Hap)–phy. ΔpH values were $\Delta pH > 0$, as expected for the basic contribution of the adsorption. The positive ΔpH was explained by the positive charge accumulation on the surface of Hap and phy at the lowest pH point.

In aqueous systems, pH dependence of adsorption has been reported [37,38] where the following adsorption mechanisms were proposed:

$$3(\equiv SO^-) + Tb^{3+} \leftrightarrow (\equiv SO)_3Tb$$

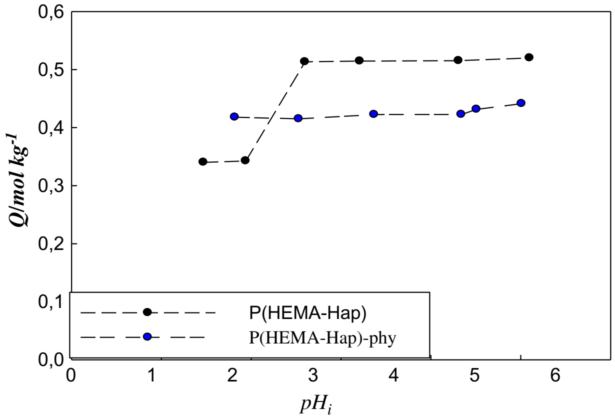

Fig. 1. The effect of initial pH values of Tb^{3+} solutions onto P(HEMA-Hap) and P(HEMA-Hap)-phy.

$$3(\equiv SO^-) + Tb(OH)^{2+} \leftrightarrow (\equiv SO)_3Tb + OH^-$$

$$3(\equiv SO^-) + Tb(OH)^{2+} \leftrightarrow (\equiv SO)_3Tb + OH^-$$

and

$$(\equiv SO^-)_3Tb + 3H^+ \leftrightarrow 3(\equiv SOH) + Tb^{3+}$$

$$\equiv SOH + H^+ \leftrightarrow \equiv SOH_2^+$$

$$\equiv SOH_2^+ + H_2O \leftrightarrow \equiv SOH + H_3O^+$$

$$\equiv SOH^+H_2O \leftrightarrow \equiv SO^- + H_3O^+$$

3.2. Concentration dependence of Tb^{3+} adsorption

The fractional transfer (F) of ^{160}Tb onto the adsorbents was calculated by using the formula:

$$F = (A_i - A_e)/A_i$$

where A_i and A_e were the activities measured in initial and equilibrium solutions. Q values (mol kg^{-1}) were then calculated using the formula: $Q = [F \times C_i \times V/w]$, C_i, the initial Tb^{3+} concentration (mol L^{-1}); w, the mass of adsorbent (kg), and V, the solution volume (L).

The Langmuir $[Q = (K_L X_L C_e)/(1 + K_L C_e)]$ and Freundlich $(Q = X_F C_e^{\beta})$ formula were used for determining adsorption capacities of the two adsorbents. Experimental data obtained fitted well to the theoretical models (Fig. 2, and Table 1).

The isotherms were also evaluated with reference to Dubinin–Radushkevich (D–R) model to determine $K_{D\text{–}R}$ (mol^2 K J^{-2}) related to the sorption energy from $Q = X_{DR}e^{-K_{D\text{–}R}\varepsilon^2}$ (Fig. 2, and Table 1). The adsorption of Tb^{3+} onto P(HEMA–Hap) and P (HEMA–Hap)–phy adsorbents and Hap corresponded to type L and H adsorption isotherms in the Giles classification. The X_L values of the P (HEMA–Hap) and P(HEMA–Hap)–phy adsorbents were found to be higher than that of Hap. This finding could indicate that the encapsulation of Hap in P(HEMA) (nonadsorbent) increased the adsorption of Tb^{3+}. This increase was attributed to the catalytic contribution of P(HEMA): the fine dispersion of mineral particles in P(HEMA) resulted in the expansion of adsorptive surfaces and numbers of active sites available for adsorption. Results obtained indicated, however, that phy modification in fact caused a substantial decrease in the adsorption capacity of the composite.

The adsorption mechanism appeared to involve a monolayer molecule adsorption. A threshold $E_{D\text{–}R}$ value of $\cong$8–16 kJ mol^{-1} was assumed for the nature of adsorption, the diffusion process seemed to involve only the physical forces as the ions did not adhere to the internal surfaces of the adsorbents (Table 1). The $E_{D\text{–}R}$ values of this investigation suggested that the process was chemical sorption [39,40].

Langmuir isotherms were further considered to predict if the adsorbents were "favorable" in view of dimensionless factor (R_L), and to calculate the weight of the adsorbents (w; kg) for removing of Tb^{3+} from hypothetic solutions with "V"(L) volume: $R_L = 1/(1 + K_L C_e)$ and $W/V = (C_i - C_e)/[K_L X_L C_e/(1 + K_L C_e)]$ as suggested [41].

The value of "R_L" from dimensionless analysis of the studied was always $0 < R_L < 1$ suggesting that the adsorbents were favourable for Tb^{3+} adsorption. The R_L values of P(HEMA–Hap), P(HEMA–Hap)–phy and Hap component for initial concentration of 100 mg L^{-1} were 0.50, 0.02, and 0.33, respectively. The sufficiency of such low amounts for Tb^{3+} removal/recovery procedures should also be considered as an evidence for the effectiveness of P(HEMA–Hap) and P(HEMA–Hap)–phy adsorbents. It was estimated that 0.5 mg L^{-1} P

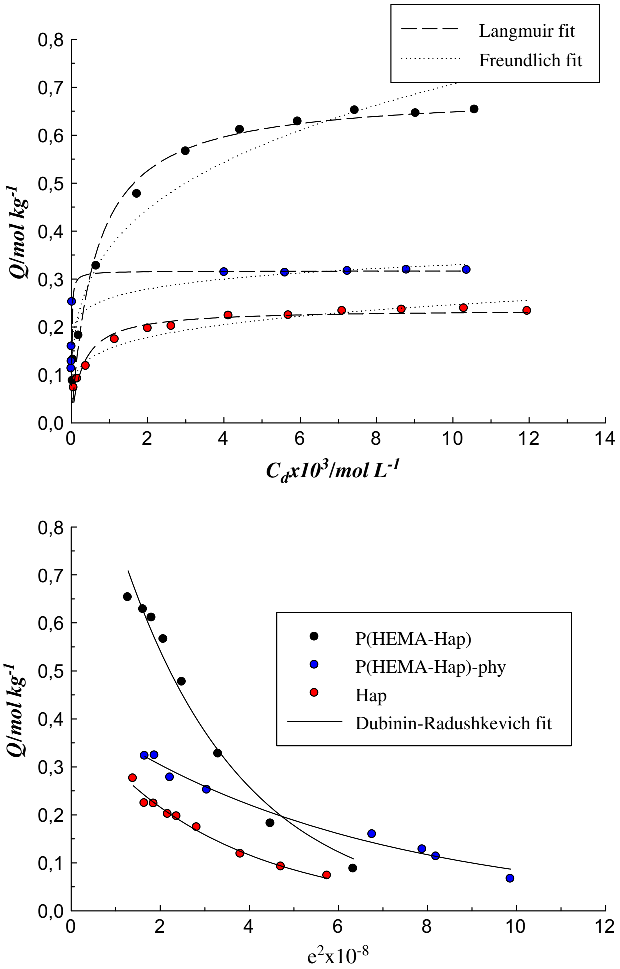

Fig. 2. Compatibility of experimentally obtained adsorption isotherms to Langmuir, Freundlich and Dubinin-Radushkevich models.

(HEMA–Hap) or P(HEMA–Hap)–phy were sufficient for the complete removal of Tb^{3+} from $100\,mg\,L^{-1}$ ion solutions.

A *t*-test was applied to obtain the significance of regression coefficients (R^2) for the compatibility of experimental data to the Langmuir, Freundlich and D–R models equations; and $p < 0.05$ was considered as the threshold for the significance [42].

3.3. Adsorption kinetics

Equations related to the pseudo-second order kinetic and intra-particle diffusion models were $t/Q_t = 1/(kQ_e^2) + t/Q_e$, and $Q_t = k_i t^{1/2}$ (Q_t and Q_e, the adsorbed amounts ($mol\,kg^{-1}$) at time t, k and k_i, rate constants). Initial adsorption rate (H) was calculated by using the equation:

Table 1
Parameters derived from the compatibility of experimentally obtained isotherms for Tb^{3+} adsorption to Langmuir, Freundlich and D–R models

	P(HEMA-Hap)	P(HEMA-Hap)-phy	Hap
Langmuir			
X_L ($mol\,kg^{-1}$)	0.69	0.31	0.24
K_L ($L\,mol^{-1}$)	1612	97750	3294
$^*R^2$	0.979	0.960	0.955
Freundlich			
X_F	2.64	0.53	0.62
β	0.29	0.10	0.20
$^*R^2$	0.957	0.878	0.943
D–R			
E ($kj\,mol^{-1}$)	11.6	17.7	12.7
$^*R^2$	0.977	0.983	0.982

*Statistically significant, $p < 0.05$.

$$H = kQ_e^2$$

which relates to the time required for adsorption of half of the concentrations ($t_{1/2}$) given by $t_{1/2} = 1/(kQ_e) = Q_e/H$ [43]. The compatibility of Tb^{3+} experimental data to the pseudo-second order kinetics and intra-particle diffusion (Weber–Morris) intra-particle diffusion models were evaluated (Table 2), with reference to the statistical significance of linearity obtained from "$t - t/Q_t$" and "$t^{0.5} - Q_t$" plots (Fig. 3 (a) and (b)).

Statistical significance of the coefficients of regressions ($p < 0.05$), indicated that the pseudo-second order model was the fitted kinetic model of adsorption. Furthermore, to the identicalness of the values of the adsorbed amounts at equilibrium obtained from the model (Q_e) and from the experiment (Q_t), confirmed the concentration dependent nature of adsorption. The correlation coefficients 0.999 and 0.997 also demonstrated that the kinetic adsorption may be defined by the pseudo-second order equation.

3.4. Temperature dependence of Tb^{3+} adsorption

To elucidate the temperature dependence of adsorption, the distribution coefficients (K_d) were derived from $K_d = Q/C_e$ for each temperature, – "ln K_d" was depicted against $1/T$ to provide adsorption

Table 2
Kinetic parameters derived from the pseudo-second order and Weber-Morris models and thermodynamic parameters for adsorption of Tb^{3+} onto the adsorbents

	P(HEMA-Hap)	P(HEMA-Hap)-phy
Pseudo second order model		
$^1k/$ (mol^{-1} kg dk^{-1})	0.28	8.04
^2Q_e (mol kg^{-1})	0.52	0.145
^2Q_t (mol kg^{-1})	0.51	0.143
$^4Hx10^2$ (mol kg^{-1} dk^{-1})	7.7	16.9
$^3t_{1/2}$ (dk)	6.7	0.9
$^*R^2$	0.999	0.997
Weber-Morris model		
$^5k_i \times 10^3$ (mol kg^{-1} $dk^{0.5}$)	4.08	0.59
$^*R^2$	0.887	0.888
Thermodynamic parameters		
ΔH (kj mol^{-1})	10.6	12.1
ΔS (j mol^{-1} K^{-1})	94	77
$-\Delta G$ (kj mol^{-1})	17.5	10.9
$^*R^2$	0.967	0.981

*Statistically significant, $p < 0.05$.

enthalpy (ΔH, kJ mol^{-1}), and entropy (ΔS, J mol^{-1} K^{-1}) from the slopes ($\Delta H/R$) and intercepts ($\Delta S/R$) of the depictions, with reference to $\ln K_d = \Delta S/R - \Delta H/(RT)$. After ΔH and ΔS values were obtained, ΔG values were calculated using the formula $\Delta G = \Delta H - T\Delta S$ for 298 K.

Temperature dependence of the adsorption of the Tb^{3+} ions was shown in Fig. 3(c). The thermodynamic parameters derived from the depictions were introduced in Table 2.

The enthalpy and entropy changes were, $\Delta H > 0$ and $\Delta S > 0$ for P(HEMA–Hap) and P(HEMA–Hap)–phy adsorbents, indicating that the adsorption process of Tb^{3+} was endothermic in the solid-solution interface. The Gibbs free energy change, $\Delta G < 0$, also proved that the adsorption process was spontaneous and the spontaneity was in favor of P(HEMA–Hap).

3.5. Reusability

The reusability of P(HEMA–Hap) and P(HEMA–Hap)–phy adsorbents were tested for Tb^{3+} for five regenerations (one initial and four repetitions). The means of for repetitive adsorptions of did not seem to be significantly different from the initial adsorption value ($p < 0.05$). Hence, the reusability tests proved that the structure of P(HEMA–Hap) and P(HEMA–Hap)–phy

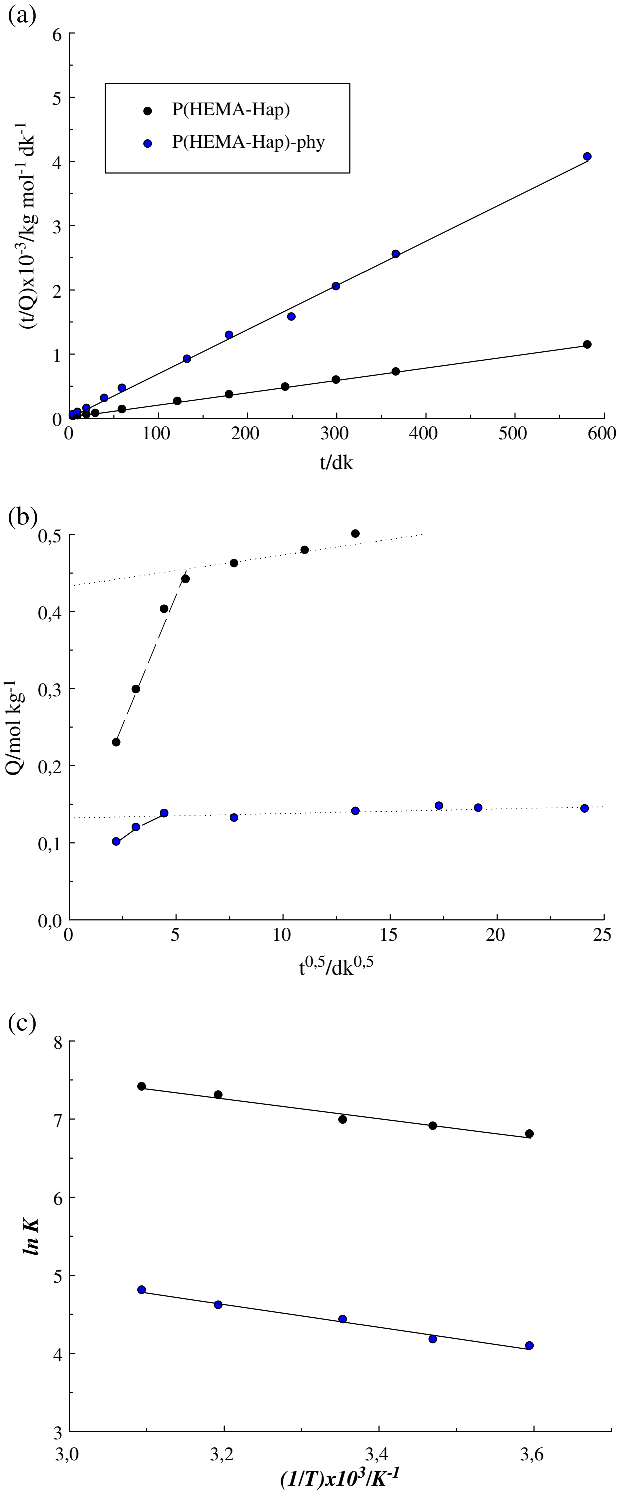

Fig. 3. The compatibility of Tb^{3+} adsorption kinetics to (a) pseudo second order (t/Q_t vs. t) and (b) Weber-Morris (Q_t vs. $t^{0.5}$) models (c) temperature dependence of adsorption.

adsorbents were not affected by the recovery/reconditioning procedures.

3.6. The effect of ionic strength

Tb^{3+} adsorption from $CaCl_2$ containing solutions (0.01–0.30 M) were in the range of 85.2–83.5 and 92.9–91.9% for P(HEMA–Hap) and P(HEMA–Hap)–phy, respectively. It was observed that the ionic strength of $CaCl_2$ solutions did not have any significant effects on the adsorption capacity of adsorbents.

4. Conclusion

In the adsorption efficiency of P(HEMA–Hap) and P(HEMA–Hap)–phy adsorbents, it was clearly shown that adsorption capacity of both P(HEMA–Hap) and P (HEMA–Hap)–phy adsorbents were much better than that of Hap for Tb^{3+}.

The compatibility of Tb^{3+} adsorption kinetics to the pseudo-second order model was chemical and it was followed by intra-particle diffusion. Free energy values derived from D–R model also confirmed the chemical nature of the process. The isotherms calculated were of *L* and *H* type. The values of enthalpy and entropy changes were positive for Tb^{3+} ions. The regeneration tests for P(HEMA–Hap) and P(HEMA–Hap)–phy showed complete recovery. Taken together, it was clearly demonstrated in this study that both P (HEMA–Hap) and P(HEMA–Hap)–phy could be used for the enrichment and separation of Tb^{3+} present in the aqueous solutions.

Acknowledgment

This work was supported by The Research Fund of Cumhuriyet University (CÜBAP) to which the author is grateful.

References

[1] C.F. Liao, Y.F. Jiao, Y. Liang, P.G. Jiang, H.P. Nie, Adsorption–extraction mechanism of heavy rare earth by Cyanex272-P507 impregnated resin, T. Nonferr. Metal. Soc. 20 (2010) 1511–1516.

[2] P. Mirezky, A.F. Cirelli, Fluoride removal from water by chitosan derivatives and composites: A review, J. Fluorine. Chem. 132 (2011) 231–240.

[3] C.H. Xiong, Y. Meng, C.P. Yao, Characters of kinetic and equilibrium of adsorption of Eu(III) by an cation exchange resin, Iran J. Chem. Chem. Eng. 30 (2011) 97–105.

[4] D.D. Li, X.J. Chang, Z. Hu, Q.H. Wang, R.J. Li, X.L. Chai, Samarium (III) adsorption on bentonite modified with N-(2-hydroxyethyl) ethylenediamine, Talanta 83 (2011) 1742–1747.

[5] P.J. Tong, Y. Liao, R.Z. Li, F. Cao, S.L. Zhao, L.L. Yang, Adsorption property of in situ immobilized black wattle tannin to La^{3+}, Pr^{3+} and Nd^{3+}, Rare Metal Mater. Eng. 40 (2011) 269–274.

[6] S. Hirano, K.T. Suzuki, Exposure, metabolism, and toxicity of rare earths and related compounds, Environ. Health Perspect. 104 (1996) 85–95.

[7] U. Ulusoy, J.E. Whitley, Profiles of faecal output of rare earth elements and stable isotopic tracers of iron and zinc after oral administration, Br. J. Nutr. 84 (2000) 605–617.

[8] R.G. Whymer, Reprocessing of nuclear fuel, In: G.R. Chopin, M.K. Khankhasayev (Eds.), Chemical Separation Technologies and Related Methods of Nuclear Waste Management, Kluwer Academic Publishers, Netherlands, 1998, pp. 29–52.

[9] H. Lippold, J. Lippmann-Pipke, Effect of humic matter on metal adsorption onto clay materials: Testing the linear additive model, J. Contam. Hydrol. 109 (2009) 40–48.

[10] Z.H. Wang, G.X. Ma, J. Lu, W.P. Liao, D.Q. Li, Separation of heavy rare earth elements with extraction resin containing 1-hexyl-4-ethyloctyl isopropylphosphonic acid, Hydrometallurgy 66 (2002) 95–99.

[11] R. Akkaya, PhD. Thesis. Preparation of bentonite/zeolite-polyhdroxyethyl methacrylate and polyacrylamide-co-maleic aicd nanocomposites and investigation fort their adsorptive features for metal ions, Cumhuriyet Üniversity, Sivas, Turkey, 2009, p. 254.

[12] N. Balkaya, T. Bektas, Chromium(VI) sorption from dilute aqueous solutions using wool, Desalin. Water Treat. 3 (2009) 43–49.

[13] B. Salih, A. Denizli, P. Kavaklı, R. Say, E. Piskin, Adsorption of heavy metal ions onto dithizone-anchored poly (EGDMA–HEMA) microbeads, Talanta 46 (1998) 1205–1213.

[14] A. Saglam, S. Bektas, S. Patır, O. Genc, A. Denizli, Novel metal complexing ligand: thiazolidine carrying poly(hydroxyethylmethacrylate) microbeads for removal of cadmium(II) and lead(II) ions from aqueous solutions, React Funct. Poly. 47 (2001) 185–192.

[15] A. Denizli, R. Say, B. Garipcan, S. Patır, Methacryloylamidoglutamic acid functionalized poly(2-hydroxyethyl methacrylate) beads for $UO_2{}^{2+}$ removal, React Funct. Poly. 58 (2004) 123–130.

[16] A. Denizli, B. Garipcan, A. Karabakan, H. Senöz, Synthesis and characterization of poly(hydroxyethyl methacrylate-N-methacryloyl-(l)-glutamic acid) copolymer beads for removal of lead ions, Mater. Sci. Eng. B-Solid 25 (2005) 448–454.

[17] M.H. Casimiro, J.P. Leal, M.H. Gil, Characterisation of gamma irradiated chitosan/pHEMA membranes for biomedical purposes, Nucl. Instrum. Methods B. 236 (2005) 482–487.

[18] B.H. Samia, L. Bousselmi, E.M. Rezrazi, P. Berçot, E. Triki, Comparative study of protective magnesium deposit behaviour obtained by continuous and pulsed currents from methylmagnesium chloride solution, Surf. Coatings Technol. 202 (2008) 3579–3584.

[19] X.B. Chen, J.V. Wright, J.L. Conca, L.M. Peurrung, Effects of pH on heavy metal sorption on mineral apatite, Environ. Sci. Technol. 31 (1997) 624–631.

[20] N.C.C. Da-Rocha, R.C. Decompos, A.M. Rossi, E.L. Moreira, A.D. Barbosa, G.T. Moure, Cadmium uptake by hydroxyapatite synthesized in different conditions and submitted to thermal treatment, Environ. Sci. Technol. 36 (2002) 1630–1635.

[21] S. Babel, T.A. Kurniawan, Low-cost adsorbents for heavy metals uptake from contaminated water: A review, J. Hazard. Mater. 3967 (2003) 1–25.

[22] E. Deydier, R. Guilet, P. Sharrock, Beneficial use of meat and bone meal combustion residue: An efficient low cost material to remove lead from aqueous effluent, J. Hazard. Mater. 101 (2003) 55–64.

[23] A. Krestou, A. Xenidis, A. Panias, Mechanism of aqueous uranium (VI) uptake by hydroxyapatite, Min. Eng. 17 (2004) 373–381.

[24] U. Ulusoy, S. Simsek, Lead removal by polyacrylamide–bentonite and zeolite nanocomposites: Effect of phytic acid immobilization, J. Hazard. Mater. 127 (2005) 163–171.

[25] V.K. Gupta, P.J.M. Carrott, M.M.L.R. Carrot, S. Suhas, Low-cost adsorbents: Growing approach to wastewater treatmenta review, Crit. Rev. Environ. Sci. Technol. 39 (2009) 783–842.

[26] Z. Talip, M. Eral, U. Hiçsönmez, Adsorption of thorium from aqueous solutions by perlite, J. Environ. Radioact. 100 (2009) 139–143.

[27] D. Bingöl, N. Tekin, M. Alkan, Brilliant yellow dye adsorption onto sepiolite using a full factorial design, Appl. Clay Sci. 50 (2010) 315–321.

[28] J. Andersson, S. Areva, B. Spliethoff, M. Linden, Sol–gel synthesis of a multifunctional, hierarchically porous silica/apatite composite, Biomaterials 26 (2005) 6827–6835.

[29] M. Czerniczyniec, S. Farías, J. Magallanes, D. Cicerone, Arsenic(V) adsorption onto biogenic hydorxyapatite: Solution composition effects, Water Air Soil Pollut. 180 (2007) 75–82.

[30] J. Pena, I. Izguierdo-Barba, A.M. Garcia, M. Vallet-Regi, Room temperature synthesis of chitosan/apatite powder and coatings, J. Am. Ceram. Soc. 26 (2009) 3631–3638.

[31] L.Q. Li, Z.Q. Chen, W.B. Darvell, Q. Zeng, G. Li, G.M. Ou, M.Y. Wu, Biomimetic synthesis of the composites of hydroxyapatite and chitosan-phosphorylated chitosan polelectrolyte complex, Mater. Lett. 60 (2006) 3553–3556.

[32] H. Kasgoz, New sorbent hydrogels for removal of acidic dyes and metal ions from aqueous solutions, Poly. Bull. 56 (2006) 517–528.

[33] R. Donat, N. Guy, H. Çetişli, Sorption isotherms and characteristics of U(VI) ion onto composite adsorbent, Desalin. Water Treat. 30 (2011) 186–194.

[34] A.A. Atia, A.M. Donia, R.A. Hussin, R.T. Rashad, Swelling and metal ion uptake characteristics of kaolinite containing poly [(acrylic acid)-co-acrylamide] hydrogels, Desalin. Water Treat. 3 (2009) 73–82.

[35] R. Akkaya, U. Ulusoy, Adsorptive features of chitosan entrapped in polyacrylamide hydrogel for Pb^{2+}, UO_2^{2+} and Th^{4+}, J. Hazard. Mater. 151 (2008) 380–388.

[36] U. Ulusoy, R. Akkaya, Adsorptive features of polyacrylamide–apatite composite for Pb^{2+}, UO_2^{2+} and Th^{4+}, J. Hazard. Mater. 163 (2009) 98–108.

[37] P. Rönnback, M. Aström, J. Gustafsson, Comparison of the behaviour of rare earth elements in surface waters, over burden ground waters and bedrock ground waters in two granitoidic settings, Appl. Geochem. 23 (2008) 1862–1880.

[38] A.A. Migdisov, A.E. Williams-Jones, T. Wagner, An experimental study of the solubility and speciation of the rare earth elements (III) in fluoride and chloride-bearing aqueous solution sat temperature sup to 300˚C, Geochim. Cosmochim. Acta 73 (2009) 7087–7109.

[39] B.S. Krishna, D.S.R. Murthy, B.S. Jai-Prakash, Thermodynamics of chromium (VI) anionic species sorption onto surfactant-modified montmorillonite clay, J. Colloid Interf. Sci. 229 (2000) 230–236.

[40] A.R. Cestari, V.F. Eunice, C.R.S. Mottos, Thermodynamics of the Cu(II) adsorption on thin vanillin-modified chitosan mebranes, J. Chem. Thermodyn. 38 (2006) 1092–1099.

[41] M. Doğan, M. Alkan, Removal of methyl violet from aqueous solution by perlite, J. Colloid Interf. Sci. 267 (2003) 32–41.

[42] J.C. Miller, J.N. Miller, Statistics for Analytical Chemistry, John Wiley & Sons, New York, NY, 1989.

[43] S.Y. Ho, G. McKay, Pseudo-second order model for sorption processes, Process. Biochem. 34 (1999) 451–465.